Molecular Biology of the Cell
Vol. 20, 282–295, January 1, 2009

Distinct Apical and Basolateral Membrane Requirements for Stretch-induced Membrane Traffic at the Apical Surface of Bladder Umbrella Cells

Weiqun Yu,*† Puneet Khandelwal,* and Gerard Apodaca*†‡

*Laboratory of Epithelial Cell Biology and Renal Electrolyte Division of the Department of Medicine, Departments of †Bioengineering, and ‡Cell Biology and Physiology, University of Pittsburgh, Pittsburgh, PA 15261

Submitted April 30, 2008; Revised October 23, 2008; Accepted October 27, 2008
Monitoring Editor: Keith E. Mostov

Epithelial cells respond to mechanical stimuli by increasing exocytosis, endocytosis, and ion transport, but how these processes are initiated and coordinated and the mechanotransduction pathways involved are not well understood. We observed that in response to a dynamic mechanical environment, increased apical membrane tension, but not pressure, stimulated apical membrane exocytosis and ion transport in bladder umbrella cells. The exocytic response was independent of temperature but required the cytoskeleton and the activity of a nonselective cation channel and the epithelial sodium channel. The subsequent increase in basolateral membrane tension had the opposite effect and triggered the compensatory endocytosis of added apical membrane, which was modulated by opening of basolateral K^+ channels. Our results indicate that during the dynamic processes of bladder filling and voiding apical membrane dynamics depend on sequential and coordinated mechanotransduction events at both membrane domains of the umbrella cell.

INTRODUCTION

Mechanotransduction, the ability of cells to sense and then respond to mechanical stimuli, depends on the polarized distribution and action of stretch-activated channels, the cytoskeleton, cell adhesion proteins including integrins, signaling molecules, and other cell-associated components that include the extracellular matrix (Ingber, 2006). These diverse elements must act in a harmonized manner to modulate mechanically responsive processes such as gene expression, cell signaling, ion transport, and membrane trafficking events such as exocytosis and endocytosis (Apodaca, 2002; Ingber, 2006). Mechanotransduction is by necessity more intricate in epithelial cells, which form cell–cell and cell–matrix interactions, and have a complex cytoarchitecture that includes distinct apical and basolateral plasma membrane domains. How mechanical stimuli that initiate at one plasma membrane domain of an epithelial cell are propagated and then coordinated with events that occur at the other cell surface to regulate processes such as ion and membrane transport is an open question.

The uroepithelium, which lines the inner surface of the bladder, ureters, and renal pelvis, is a useful model to study epithelial mechanotransduction. The outermost layer of this tissue is lined by a single layer of polarized umbrella cells, which are known to respond to mechanical stimuli by augmented ion transport and membrane traffic (Lewis and de Moura, 1982; Truschel *et al.*, 2002; Wang *et al.*, 2003b); however, the relationship of these two processes and the mechanical force (stretch and/or pressure) that acts upon the umbrella cell to stimulate these events is not well understood.

When isolated uroepithelial tissue is experimentally bowed outward toward its serosal surface (mimicking bladder filling) the umbrella cells increase their apical surface area in a two-stage manner. The initial "early" stage may occur in response to a changing mechanical environment and is characterized by relatively rapid increases in surface area. In the subsequent "late" stage, which occurs after the tissue has reached a mechanical equilibrium, the surface area increases slowly over several hours (Balestreire and Apodaca, 2007). The late stage is temperature sensitive and is dependent on purinergic signaling pathways, activation of the EGF receptor, and protein synthesis and secretion (Truschel *et al.*, 2002; Wang *et al.*, 2003a, 2005; Balestreire and Apodaca, 2007). In contrast, the early stage is largely unexplored but appears to be insensitive to temperature and does not require EGF signaling or protein synthesis (Balestreire and Apodaca, 2007). In addition to stimulating apical exocytosis, mechanical stimuli also trigger increased endocytosis, which modulates the increase in apical surface area (Truschel *et al.*, 2002); however, the relationship of the endocytic and exocytic events and the mechanisms by which they are initiated and coordinated is not known. Previous studies showed that the electrophysiological responses of the uroepithelium are dependent on the direction the tissue is bowed (Ferguson *et al.*, 1997); however, the physiological significance of these differences and the role of the distinct surface domains of umbrella cells in mechanotransduction is yet to be defined.

This article was published online ahead of print in *MBC in Press* (http://www.molbiolcell.org/cgi/doi/10.1091/mbc.E08–04–0439) on November 5, 2008.

Address correspondence to: Gerard Apodaca (gla6@pitt.edu).

Abbreviations used: ENaC, epithelial sodium channel; I_{sc}, short-circuit current; NSCC, nonselective cation channel; TEV, transepithelial voltage.

The goals of our study were to further explore the early stage described above, identify the mechanical stimulus that initiates exocytosis and endocytosis in umbrella cells, and understand the mechanotransduction pathways that coordinately regulate these processes. We observed that increased apical membrane tension, but not pressure, was the relevant mechanical stimulus that regulated ion transport and exocytosis at the apical surface of the umbrella cell layer. Although exocytosis was stimulated by increased apical membrane tension, the added membrane was recovered by a compensatory endocytosis that was stimulated by increased basolateral membrane tension. Further study revealed that likely mechanotransducers in the apical membrane included the apically distributed epithelial sodium channel (ENaC) and a nonselective cation channel (NSCC), whereas K^+ channels may modulate events at the basolateral surface of the cell. Our results provide evidence that in response to a dynamic mechanical environment, such as that observed during bladder filling and voiding, the apical membrane dynamics of umbrella cells are governed by sequential and coordinated mechanotransduction events at its distinct apical and basolateral membrane domains.

MATERIALS AND METHODS

Materials, Reagents, and Animals

Unless described otherwise all reagents and chemicals were obtained from Sigma (St. Louis, MO). Anti-chicken Kir6.1 antibody CAF-1 was raised against a peptide corresponding to residues 20–31 of the Kir6.1 N-terminus (ENLRKPRIRDRLP) and was kindly provided by Dr. Coetzee (New York University). It was used at a 1:400 dilution for Western blot analysis and a 1:200 dilution for immunofluorescence. Female New Zealand white rabbits (3–4 kg) were obtained from Myrtle's Rabbitry (Thompson Station, TN), C57BL/6J mice (3–4 mo old) were obtained from the Jackson Labs (Bar Harbor, ME), and Sprague Dawley rats (weighing 250–300 g) were obtained from Harlan (Indianapolis, IN). All animal studies were approved by the University of Pittsburgh Animal Care and Use Committee.

Isolation and Mounting of Uroepithelial Tissue

The preparation and mounting of rabbit uroepithelium in Ussing stretch chambers was performed as described previously (Wang *et al.*, 2003a); however, we used two closed Ussing stretch chambers in our analysis. The tissue was bowed slightly inward during the equilibration period.

Mechanical Stretch of Tissue

Tissue manipulations are shown graphically in Figure 1. Control tissue was left at 37°C and was not exposed to mechanical stimuli (see Figure 1A). In some experiments tissue was bowed outward by attaching 4-mm diameter Tygon tubing to the top Luer fitting of the mucosal hemichamber. The tubing, filled with Krebs buffer (110 mM NaCl, 5.8 mM KCl, 25 mM $NaHCO_3$, 1.2 mM KH_2PO_4, 2.0 mM $CaCl_2$, 1.2 mM $MgSO_4$, and 11.1 mM glucose, pH 7.4) that was gassed with 95% air/5% CO_2, was placed at the indicated height above an additional piece of tubing (filled with Krebs buffer) that was attached to the serosal hemichamber. The free end of the mucosal tubing was attached to a master stopcock. At the start of the experiment the master stopcock was opened, which allowed the back pressure in the mucosal hemichamber to be increased in a stepwise manner by raising the height of the mucosal tubing 4–64 cm H_2O above the starting point (Figure 1B). In some experiments the tubing attached to both hemichambers was simultaneously raised to increase pressure in both hemichambers to 4–64 cm H_2O (Figure 1C). To stretch the uroepithelium in the absence of pressure change, a filament (silk surgical suture thread) was sutured onto a 2.5-mm-diameter pad of muscle left on the serosal surface of the tissue during dissection. A 1 cm H_2O pressure head was maintained in each chamber, and the filament, threaded through the side port of the serosal hemichamber, was attached to an NE-1600 syringe pump (New Era Pump Systems, Farmington, NY) and pulled at a constant speed of 0.1–2.0 cm/min (Figure 1D). In some experiments the tissue was bowed outward (Figure 1E) or inward (Figure 1F) to discrete pressure heads of 1–16 cm H_2O using a setup similar to that described for Figure 1B. According to LaPlace's law (where T = PR/2) the tension (T) inside a spherical wall will increase proportionally to the pressure (P) and the radius of curvature (R). Assuming the degree of tissue bowing is similar, which is generally true in our system at all pressure heads examined, then changing the pressure will increase tension in the tissue. In other experiments we maintained a constant pressure head of 2 cm H_2O in the mucosal hemichamber, but changed the rate of filling by attaching different gauge needles to the end of the tubing feeding the mucosal hemichamber (Figure 1G). According to Poiseuille's law, where $dV/dt = \pi/8(R^4/\eta)(dP/L)$, if the length of the needle (L) is kept constant then the filling rate (dV/dt) will be dependent on the pressure difference (dP), the radius of the needle (R), and the viscosity of the Krebs buffer (η). Changing R (by using different gauge needles), while maintaining the other parameters constant will only change the filling rate.

Electrophysiological Data Acquisition and Capacitance Measurements

Transepithelial voltage (TEV) and membrane capacitance (where 1 μF $\approx$ 1 cm^2 of surface area) were measured as described previously (Lewis and Hanrahan, 1990; Wang *et al.*, 2003a,b); however, the voltage response was fit to a single exponential using Prism software (GraphPad Software, San Diego, CA). The fits had R^2 values of $\geq$0.98. I_{sc} was calculated by dividing the TEV by the transepithelial electrical resistance (TER; Lewis and de Moura, 1984).

Measurement of Exocytosis and Endocytosis at the Apical Surface of Umbrella Cells

Tissue was mounted and equilibrated as described and then cooled to 4°C for 30 min. After incubating apical surface of umbrella cells with freshly prepared sulfo-n-hydroxy succinimide (NHS)-acetate (1 mg/ml; dissolved in ice-cold Krebs buffer) for 60 min, the tissue was washed with ice-cold Krebs buffer, treated with 1 M lysine-HCl dissolved in Krebs buffer (the pH was adjusted to 7.4) for 5 min, and then washed again with Krebs buffer. The tissue was then stretched by increasing the mucosal pressure head to 2 cm H_2O and filling the mucosal hemichamber using a 20-gauge needle for either 5 min at 37°C or 10 min at 4°C. The apical surface of tissue was then incubated with freshly prepared sulfo-NHS-biotin (1.0 mg/ml; dissolved in Krebs buffer) for 15 min to biotinylate newly inserted apical membrane proteins. Tissue without stretch served as control. The uroepithelium was washed with ice-cold Krebs, treated with 1 M lysine-HCl/Krebs for 5 min, rinsed with Krebs buffer, and then removed from the chamber. The uroepithelium was recovered by scraping and then lysed in 0.5% SDS lysis buffer (0.5% wt/vol SDS, 100 mM triethanolamine, pH 8.6, 0.5 mM EDTA, 1 mM phenylmethylsulfonyl fluoride, 5 μg/ml leupeptin, 5 μg/ml antipain, and 5 μg/ml pepstatin). The lysate was incubated at 95°C for 5 min, vortex-shaken for 15 min, and then microfuged at 20,000 $\times$ *g* for 5 min at room temperature. Equal amounts of protein (25–50 μg) from the tissue lysates were resolved SDS-PAGE, and proteins were transferred and probed with streptavidin-HRP as described previously (Truschel *et al.*, 2002).

To measure endocytosis, tissue was mounted, equilibrated, and cooled to 4°C for 30 min. FITC-wheat germ agglutinin (WGA; 50 μg/ml) was then added to the mucosal chamber and incubated for 30 min, and the tissue was stretched for 10 min using a 20-gauge needle at a 2 cm H_2O pressure head. Tissue was then fixed, prepared, and stained with rhodamine phalloidin and Topro-3 as described previously (Truschel *et al.*, 2002). Unstretched tissue served as control.

RT-PCR Analysis

Bladders were excised from killed mice, the uroepithelium was recovered by scrapping and was RNA-purified, and RT-PCR performed as described previously (Balestreire and Apodaca, 2007).

Primers Used for PCR of K^+ Channels

The following primers (5′-3′), were used to PCR the K^+ channels with the expected product size in base pairs in parentheses, followed by the sequence: KCNMA1 (BK) CGTACTGGGAATGTGTCTACTT (223) and ACTACAATGTGCTTTCTTCCAC; KCNN1 (SK1) GGCTTTTCTTCAGGATCTATCT (171) and GTGTCCTTACTTTGACATCAGG; KCNN2 (SK2) ATCCCATACCTGGGAATTATAC (203) and TATCTTATTAAGTGCCCCAATG; KCNN3 (SK3) ACCTACGAGCGTATCTTCTACA (219) and ATCAGTGAAGAGTTTGCTATGG; KCNN4 (IK1) CACAGAAGAACCAGGCTAAGTA (219) and CTGATGAGGGCATATGTGTAGT; KCNK2 (TREK-1) AAAGGGAAAGCAAATAGAAAAC (206) and AGCATTCAGATTCATTCATAGG; KCNK4 (TRAAK) GGCGTCTCTTTTGTATCTTCTA (221) and GAAGGTAGGAGTGAGGACAAA; KCNK10 (TREK-2) AAGAGAAGAAAGAGGACGAGAC (201) and ACACATAGTCCAATTCCAATGT; KCNJ8 (Kir6.1) AACTCCATCAGGAGGAATAACT (225) and CAATATTTTGATCATCGGAACT; KCNJ11 (Kir6.2) CAAATGATTGGAGACCTTTCTA (168) and ATCCAGGTATATCAGTGTTTGC.

Western Blot and Immunofluorescence

Rat uroepithelial cells were isolated by gentle scraping, lysed in SDS lysis buffer, resolved by SDS page, and subjected to Western blot analysis as described previously (Truschel *et al.*, 2002). Rat tissue was prepared for immunofluorescent labeling as described previously (Truschel *et al.*, 2002); however, tissue was fixed in 10% (vol/vol) acetic acid, 40% (vol/vol) ethanol in phosphate-buffered saline for 40 min at 4°C. Images were acquired using a Leica TCS-SL scanning-laser confocal microscope (Deerfield, IL) as described previously (Truschel *et al.*, 2002).

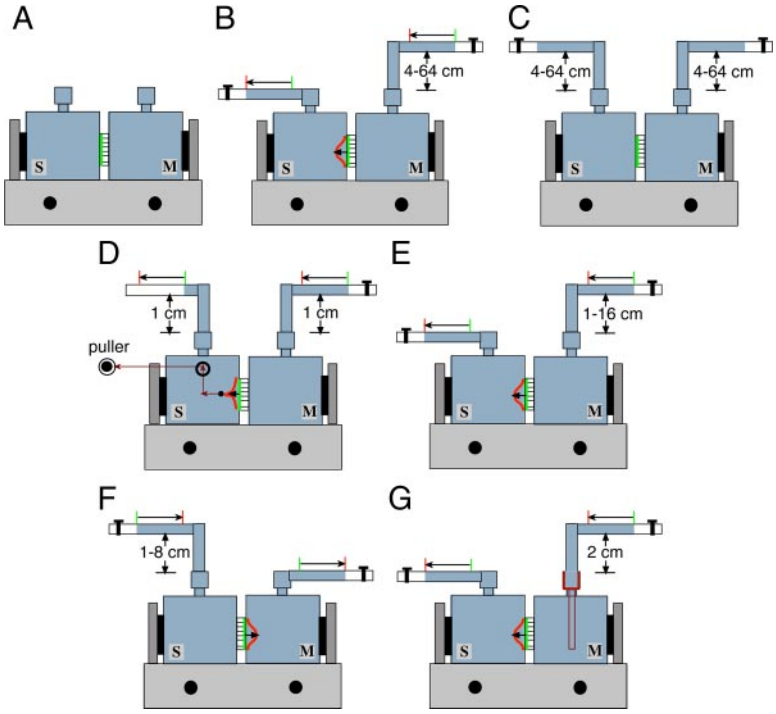

Figure 1. System for stretching the uroepithelium. Uroepithelial tissue was mounted between two closed Ussing stretch chambers, the chambers were filled with Krebs buffer, and the tissue was equilibrated for 30–45 min. (A) Control tissue was not exposed to mechanical stimuli. (B) Tissue was bowed outward in response to stepwise increases in the hydrostatic pressure head. (C) Hydrostatic pressure was simultaneously raised stepwise in both mucosal and serosal hemichambers. (D) Both the mucosal and serosal hemichambers were maintained at 1 cm H_2O pressure, and the tissue was pulled by a filament toward the serosal hemichamber. (E) Tissue was bowed outward in response to raising hydrostatic pressure in the mucosal hemichamber. (F) Tissue was bowed inward in response to raising hydrostatic pressure in the serosal hemichamber. (G) Tissue was bowed outward as the mucosal hemichamber was filled at different rates. M, mucosal hemichamber; S, serosal hemichamber. The green line between the chambers shows the initial position of uroepithelium and the red curve shows the position of the tissue upon bowing.

Statistical Analysis

Data were analyzed using Student's *t* test, and $p < 0.05$ was taken as significant. When comparing multiple samples ANOVA was performed using Bonferroni's correction.

RESULTS

Stretch, But Not Hydrostatic Pressure, Stimulates Ion Transport and Membrane Turnover in Umbrella Cells

To determine which mechanical force(s), pressure or stretch, stimulated ion transport and membrane traffic in the umbrella cells, we used isolated uroepithelium mounted in Ussing stretch chambers. In control experiments the tissue was equilibrated for 30 min (Figure 1A) and then left unperturbed for up to 3 h, during which time the umbrella cells maintained a relatively stable TEV of −15 to −20 mV, a transepithelial conductance of ~0.05 mS/cm^2 (where conductance is the inverse of transepithelial resistance), a low short-circuit current (I_{sc}) of ~2 μA/cm^2, and a transepithelial membrane capacitance (C_T) of ~2.0 μF, where 1 μF ≈ 1 cm^2 of surface area (Figure 2A). We previously showed that increases in capacitance are a result of increased apical membrane exocytosis of subapical discoidal/fusiform vesicles (Truschel *et al.*, 2002; Khandelwal *et al.*, 2008). When hydrostatic pressure in the mucosal chamber was raised to 4 cm H_2O (Figure 1B), the tissue visibly bowed outward (data not shown), and electrophysiological changes consistent with ion transport were observed including a rapid decrease in TEV and transient increases in conductance and I_{sc} (Figure 2A). Further increasing the hydrostatic pressure in the mucosal hemichamber to 8, 16, 32, or 64 cm in a stepwise manner did not induce further changes (Figure 2A), indicating that once the tissue was bowed outward further changes in hydrostatic pressure had no effect on these parameters. The C_T increased as the pressure head was raised to 4 cm H_2O and slowly rose during the next 150 min. Next, we simultaneously raised the pressure head in both the mucosal and serosal hemichambers (Figure 1C), which prevented tissue bowing, but allowed for pressure to be increased to 4, 8, 16, 32, or 64 cm H_2O against both surfaces of the tissue. Intriguingly, no change in any of the electrical parameters was noted (Figure 2A), indicating that it was increased stretch (and the resulting bowing of the epithelium) and not changes in hydrostatic pressure that induced electrophysiological changes in the umbrella cell layer.

To further confirm that stretch is the relevant mechanical force in umbrella cells, the following experiment was performed. A suture thread was attached to a small pad of muscle that was left on the serosal surface of the tissue during the dissection of the uroepithelium, and the thread pulled at different speeds (0.1, 0.5, 1.0, or 2.0 cm/min) while maintaining a constant hydrostatic pressure (1 cm H_2O; Figure 1D). Slow speeds of pulling induced relatively gradual changes in the electrophysiological properties, while rapid pulling induced quick changes (Figure 2B). Regardless of speed, we observed that stretch was accompanied by TEV hyperpolarization, and increases in conductance, I_{sc}, and C_T. The release of stretch was accompanied by a rapid return of the parameters to near baseline values, indicating that the tissue was not disrupted by the treatment. In summary, our data indicate that stretch, but not hydrostatic pressure, is the mechanical force responsible for stimulating events in the umbrella cell layer.

Umbrella Cell Electrophysiological Properties Are Sensitive to the Direction, Magnitude, and Rate of the Applied Force

In the next experiments we examined the responses of tissue that was bowed outward toward the serosal hemichamber or bowed inward toward the mucosal hemichamber. We theorized that as the mucosal hemichamber is filled, tension in the apical plasma membrane of the umbrella cells would increase first (Figure 3A). This increase in tension would be dissipated to some extent by the ability of the umbrella cell to increase its apical surface area, as well as by outward

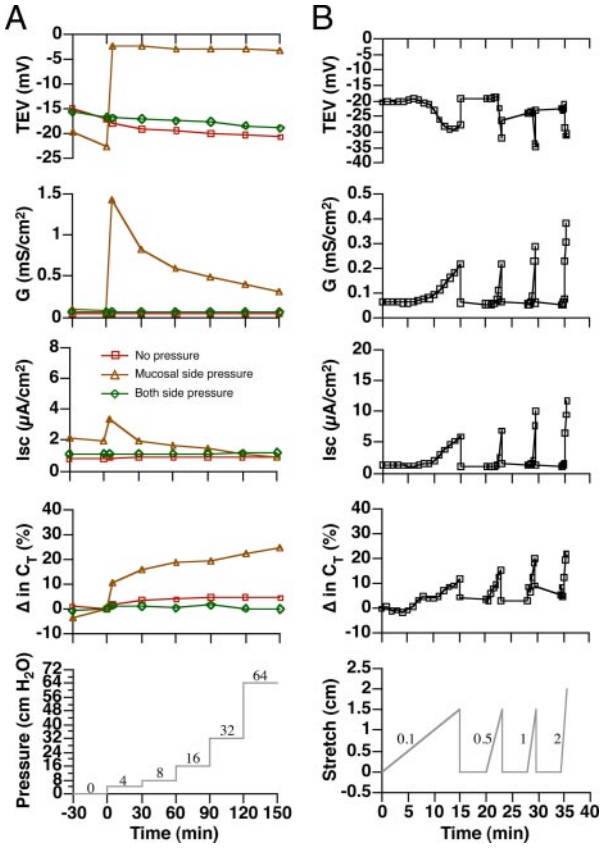

Figure 2. Modulation of electrophysiological parameters in response to mechanical stimuli. (A) Responses in tissue exposed to stepwise increases in pressure. (B) Responses to pulling the tissue toward the serosal hemichamber under constant pressure. The experiments were repeated ≥3 times, and representative results are shown.

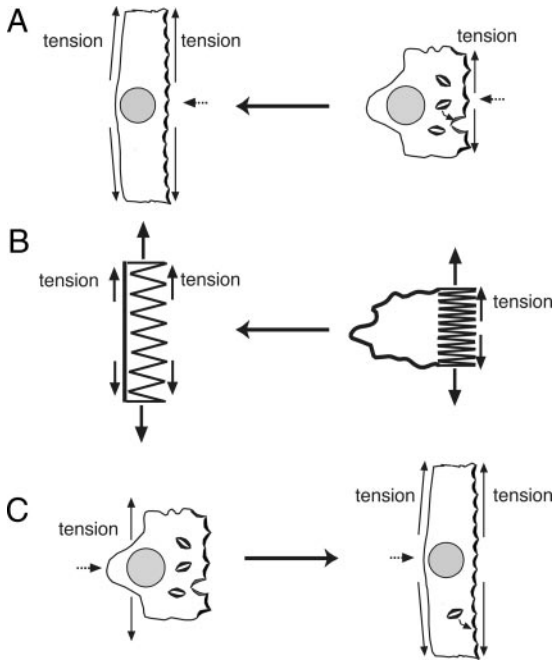

Figure 3. Mechanical and morphological features of distended umbrella cells. (A) In response to filling the mucosal hemichamber, tension initially develops in the apical membrane, which causes the tissue to bow outward. The apical membrane tension can be dissipated in part by increased exocytosis. Subsequently, tension increases in the basolateral membrane, which unlike the apical membrane does not accommodate increased tension by modulating surface area. (B) The apical membrane acts like a spring that can accommodate heightened tension by increasing apical surface area, but the spring is limited by the basolateral membrane, which may act like a rope to further constrain tension release (in the case of the umbrella cell by promoting endocytosis of apical membrane). (C) In response to filling the serosal hemichamber, tension is increased in the basolateral membrane, which causes the tissue to bow inward. As the tissue bows further, tension increases in the apical membrane.

bowing of the tissue (Figure 3B). As the stretch increases further one would expect the basolateral surface to also experience increased tension (Figure 3A). However, the ability of the basolateral membrane to accommodate tension would be constrained by its apparent lack of surface area change in response to stretch (Lewis and de Moura, 1982; Truschel *et al.*, 2002). In a reciprocal manner, bowing the tissue inward by increasing the pressure head in the serosal hemichamber would increase tension in the basolateral membrane initially, but would eventually increase apical membrane tension if the tissue was further stretched toward the mucosal hemichamber (Figure 3C).

In our previous experiments the exocytic response was monitored on the minute-to-hour time scale for up to 5 h (Truschel *et al.*, 2002; Wang *et al.*, 2003a; Balestreire and Apodaca, 2007). However, in the following experiments we sampled C_T on the second-to-minute time scale to capture the early stage events with improved resolution. When tissue was bowed outward in response to a 2 cm H_2O pressure head (Figure 1E), we observed responses that were temporally separated into three phases. In the first phase the TEV hyperpolarized, the conductance and I_{sc} increased, and the C_T increased to ~100% over starting values (Figure 4A). Because ion transport across the apical membrane of the umbrella cell is the primary contributor to transepithelial conductance (Lewis *et al.*, 1977), and because C_T increased, the changes we observed in phase 1 likely reflected increased ion transport and membrane traffic at the apical plasma membrane domain of the umbrella cells. During the second phase of outward bowing the C_T, I_{sc}, and TEV rapidly reversed course (Figure 4A). The decrease in C_T is consistent with our previous finding that in addition to stimulating exocytosis stretch also increases endocytosis, with the net effect being membrane addition (Truschel *et al.*, 2002). The decrease in I_{sc} may reflect the internalization of ion channels, changes in their open probability, or changes in the electrochemical gradients across the epithelium. By 5 min and beyond (phase 3) the tissue had reached a mechanical equilibrium and the late stage response was observed, which was characterized by a slow increase in C_T and decreases in conductance, I_{sc}, and TEV (Figure 4A).

The reversal in parameters that we observed during the second phase of outward bowing likely occurs in response to increased tension in the basolateral membranes of the umbrella cells. This possibility became apparent when we used the setup in Figure 1F to raise the pressure head in the serosal hemichamber to 1 cm H_2O. Under these conditions, the first phase of inward bowing (like the second phase of outward bowing) resulted in a decrease in TEV, I_{sc}, and C_T (compare these parameters in Figure 4, A and B). The decrease in C_T was larger during phase 2 of outward bowing, possibly reflecting changes in cellular responses when endocytosis is

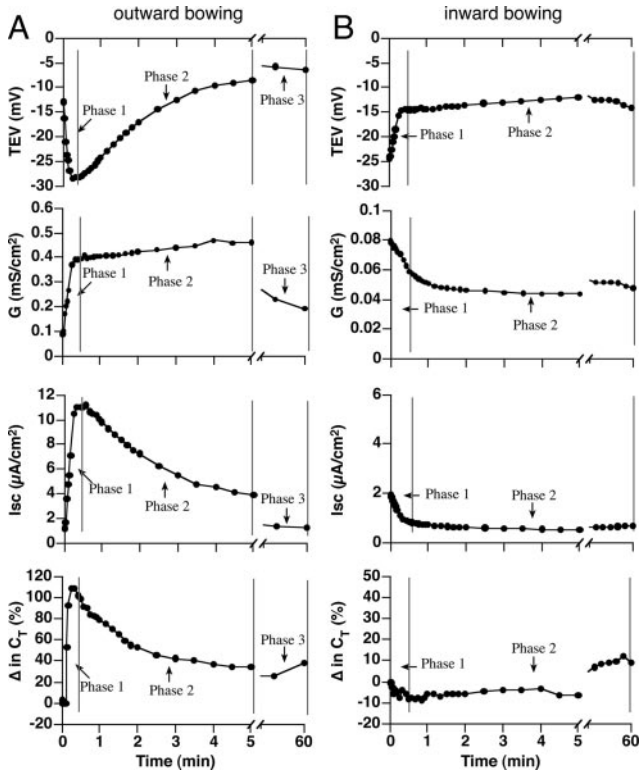

Figure 4. Modulation of umbrella cell electrophysiological parameters by changes in the direction of the mechanical force. (A) Responses in tissue bowed outward by a 2-cm H_2O pressure head in the mucosal hemichamber. (B) Responses in tissue bowed inward by a 1-cm H_2O pressure head in the serosal hemichamber. The experiments were repeated ≥3 times, and representative results are shown.

preceded by an exocytic burst. After phase 1 of inward bowing, the tissue reached an equilibrium (phase 2) in which the electrical parameters remained relatively constant (Figure 4B). In summary, apical membrane tension resulted in increased ion transport and apical membrane exocytosis, whereas increased basolateral membrane tension led to decreased I_{sc} and increased apical membrane endocytosis.

If our dual-membrane model was correct, then we expected that the responses to apical membrane tension would be limited, regardless of pressure head, by responses to the increased tension in the basolateral membrane (Figure 3B). In fact, the peak values for many of the electrophysiological parameters were similar irrespective of the magnitude of the mucosal pressure head (1–16 cm H_2O; Figure 5A and Table 1). The increased pressure not only changes the magnitude of the force but according to Poiseuille's Law (which relates changes in pressure to rates of fluid flow; see *Materials and Methods*), higher pressures induce more rapid rates of chamber filling (and vice versa). In turn, faster rates of chamber filling would act to more quickly increase membrane tension and tissue bowing. In fact we observed that the phase 1 response to 8 cm H_2O was complete in ~0.02 min (see inset in Figure 5A), but took a full minute to peak in tissue exposed to a pressure head of 1 cm H_2O (Figure 5A).

Next, we maintained a constant pressure head in the mucosal hemichamber (2 cm H_2O), and then varied the rate of buffer flow into this hemichamber by inserting different gauge needles between the end of the tubing and the Luer port at the top of the mucosal hemichamber (Figure 1G). Consistent with the hypothesis that the rate of filling (and rate of tissue bowing/stretch) will affect the kinetics of the filling response, we observed that use of an 18-gauge needle, which allows a relatively rapid flow rate of ~ 3400 μl/min, resulted in rapid changes in the electrophysiological parameters during phase 1 and 2 (Figure 5B and Table 1). In contrast, when we filled the chamber with a 25-gauge needle (flow rate of ~65 μl/min), we observed gradual changes in electrophysiological responses and a dramatic increase in the length of the phase 1 response (see inset in Figure 5B). Under these conditions the phase 2 response was only observed after ~15 min (see inset in Figure 5B). By multiplying the maximum response time (end of phase 1) by the corresponding filling rate, a relative constant value of ~1 ml was obtained, indicating a constant fill volume was needed to fully stretch the umbrella cells. Regardless of filling speed, the magnitude of the responses was similar. These data provide further evidence in support of our two-membrane model and demonstrate that the timing of the responses was dependent on a dynamic mechanical environment and the speed of tension development across the apical and then basolateral membrane domains of the umbrella cell.

We also monitored the electrophysiological parameters when the tissue was bowed inward at different pressure heads (Figure 5C). Similar responses to a 1 cm H_2O pressure head were observed at 2 cm H_2O pressure. In contrast, at 8 cm H_2O we observed a complex response. Initially, there was a change similar to that described for 1 or 2 cm H_2O (decreased TEV, I_{sc}, and C_T). However, the subsequent response was similar to that observed when apical membrane tension was increased: an increase then decrease in TEV, the conductance decreased and then increased, and the I_{sc} and C_T gradually increased (Figure 5C). As proposed in Figure 3C, the response to 8 cm H_2O likely resulted from the initial increase in tension at the basolateral membrane followed by a subsequent increase in apical membrane tension, which we showed stimulated ion transport and apical exocytosis. These data are consistent with the idea that tension can develop in a sequential manner when the tissue is bowed in either direction.

Stretch Stimulates Rapid Membrane Turnover at the Apical Surface of Umbrella Cells, Which Is Dependent on the Cytoskeleton

An intriguing finding in our analysis was that rapid changes in membrane tension were accompanied by rapid and relatively large increases in C_T. Consistent with our previous findings (Balestreire and Apodaca, 2007), the change in C_T observed during phase 1 was insensitive to the secretory inhibitor brefeldin A (BFA; Table 1), whereas the change in C_T was significantly inhibited at time points >60 min (data not shown). To confirm that the phase 1 response reflected real changes in exocytosis at the apical surface of the umbrella cells, we initially assessed whether C_T was sensitive to incubation at 4°C, a temperature routinely used to block exocytosis and endocytosis in quiescent cells. Surprisingly, the initial change in C_T (at the end of phase 1) was similar at 37 or 4°C (Table 1). The lower temperature did alter the change in C_T observed during the phase 3 response (Table 1).

To further confirm these findings, we used a biotinylation approach to show that exocytosis was stimulated during phase 1, and this increase occurred in a temperature-independent manner (Figure 6, A–D). We first blocked the majority of NHS-reactive groups on the apical surface of quiescent umbrella cells using NHS-acetate (up to 2 mg/ml), a

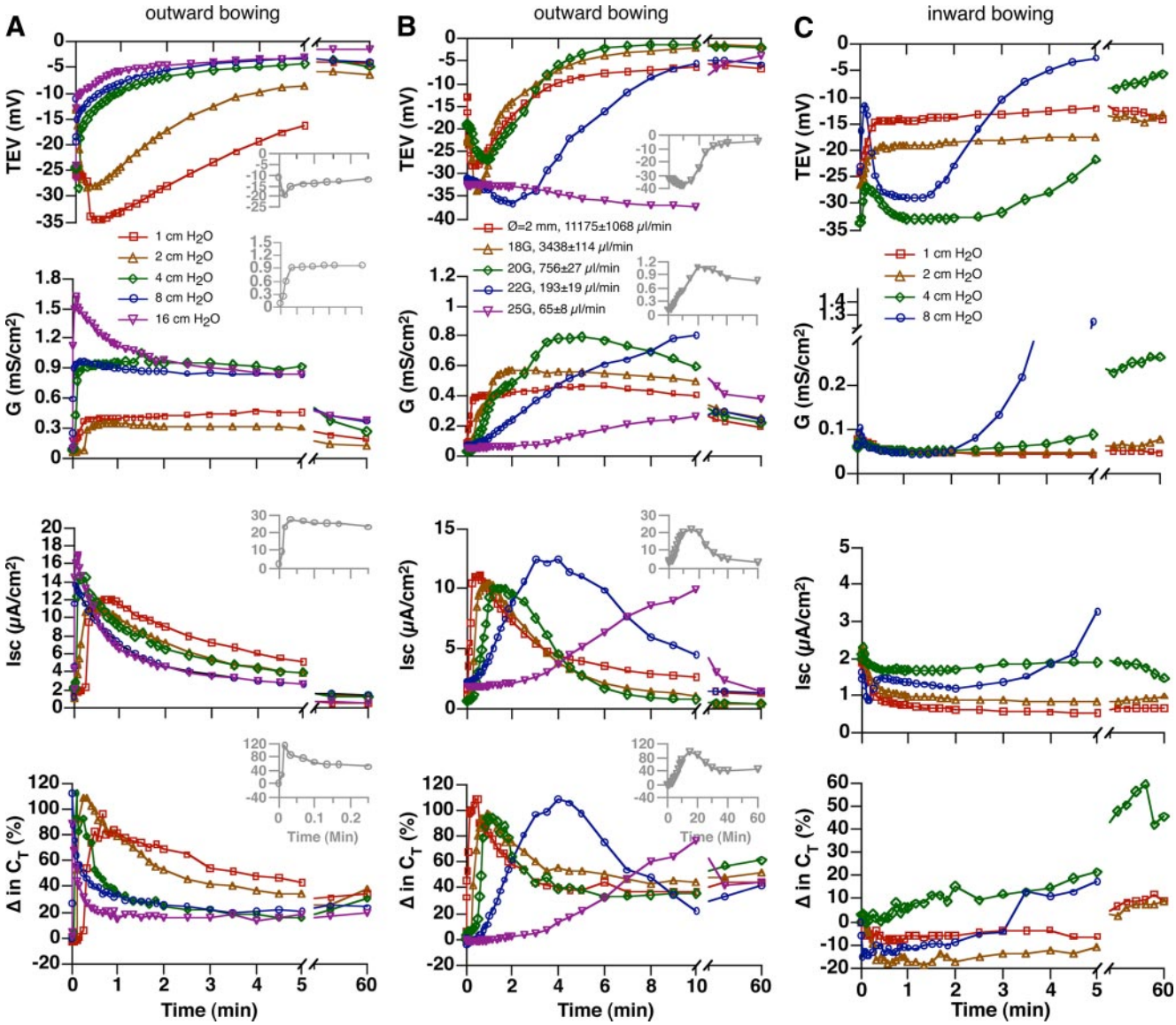

Figure 5. Electrophysiological responses to different pressure heads and rates of chamber filling. (A) Effect of different pressure heads on electrophysiological parameters as the tissue was bowed outward. Insets show responses observed when the hydrostatic pressure was raised to 8 cm H_2O. (B) Responses to different rates of filling when the pressure head was maintained at 2 cm H_2O in the mucosal hemichamber. The legend shows the gauge of needle and approximate rate of filling. The insets show data for the 25-gauge needle. (C) Effect of different pressure heads on electrophysiological parameters as the tissue was bowed inward. The experiments were repeated ≥3 times and representative results are shown. Data for the responses to 2 cm H_2O (outward bowing) and 1 cm H_2O (inward bowing) are reproduced from Figure 4.

treatment that effectively prevented apical membrane proteins from being subsequently labeled with an NHS-S–S-biotin reagent (Figure 6A). Next, the tissue was bowed outward and was incubated for either 5 min at 37°C (Figure 6B) or for 10 min at 4°C (Figure 6C). We reasoned that if stretch stimulated increased exocytosis, then new proteins would appear at the cell surface and expose new reactive groups that could be identified using the NHS-S–S-biotin reagent. Indeed, we observed a significant increase in the surface expression of several protein species both at 37 and 4°C (Figure 6, B and C), confirming that exocytosis occurred under these conditions. In addition to exocytosis, we also observed that FITC-labeled wheat germ agglutinin was endocytosed when the tissue was stretched at 4°C (Figure 6F), but endocytosis was not observed in control tissue not exposed to mechanical stretching (Figure 6F).

It was previously observed that umbrella cell exocytosis depends on the actin cytoskeleton (Lewis and de Moura, 1982). We assessed whether exocytosis was observed in tissue that was pretreated with cytochalasin D for 60 min before stretch. Under these conditions we observed that C_T was significantly decreased (Figure 7 and Table 1), and the surface expression of proteins was not increased in response to stretch (Figure 6D). We noted that the protein pattern in tissue pretreated with cytochalasin D was different from that observed in untreated tissue. This difference likely reflects alterations in protein distribution during the cytochalasin pretreatment. We also observed that the actin depolymeriz-

Table 1. Effect of various treatments on C_T

Experimental manipulation	n	C_{max} (%)	C_{min} (%)	C_{60} (%)
Force magnitude				
1 cm H_2O	3	101.6 ± 10.9	29.6 ± 1.2	38.6 ± 6.9
2 cm H_2O[a]	3	99.3 ± 9.6	30.0 ± 3.6	35.0 ± 4.9
4 cm H_2O	3	115.0 ± 13.6	20.0 ± 2.3	25.3 ± 2.0
8 cm H_2O	3	107.6 ± 14.4	18.3 ± 0.8	26.6 ± 3.1
16 cm H_2O	3	89.6 ± 2.9	15.3 ± 0.8	18.6 ± 0.3
Fill speed				
2 cm H_2O/2 mm[a]	3	99.3 ± 9.6	30.0 ± 3.6	35.0 ± 4.9
2 cm H_2O/18 g	4	93.0 ± 4.8	38.0 ± 1.6	51.7 ± 0.7
2 cm H_2O/20 g[b]	7	106.2 ± 9.6	35.0 ± 3.7	51.5 ± 5.6
2 cm H_2O/22 g	3	95.7 ± 13.5	25.7 ± 5.5	50.0 ± 7.0
2 cm H_2O/25 g	3	88.3 ± 7.6	36.0 ± 5.6	50.3 ± 6.1
Temp or BFA				
Control[b]	7	106.2 ± 9.6	35.0 ± 3.7	51.5 ± 5.6
4°C	5	100.0 ± 4.6	36.5 ± 4.6	20.0 ± 4.4*
BFA	3	104.6 ± 8.3	24.6 ± 0.3	28.0 ± 0.5
Cytoskeleton disruptors				
Cytochalasin D	4	38.2 ± 4.1*	21.2 ± 4.8	43.7 ± 4.0
Latrunculin A	3	71.0 ± 4.5	33.3 ± 5.2	58.0 ± 6.6
Colchicine	3	99.6 ± 10.4	36.0 ± 6.8	46.3 ± 2.3
Thioglycolate	4	53.2 ± 5.2*	30.5 ± 5.2	51.0 ± 8.0
Okadaic acid	4	43.0 ± 7.0*	29.0 ± 3.8	36.7 ± 4.9
Channel blockers				
Gd_3Cl, mucosal	4	47.0 ± 3.3*	28.2 ± 3.7	45.0 ± 8.9
La_3Cl, mucosal	3	65.3 ± 10.6*	25.6 ± 2.9	40.0 ± 3.7
100 μM amiloride, mucosal	3	44.3 ± 2.1*	30.3 ± 3.3	45.6 ± 3.8
1 μM amiloride, mucosal	4	42.2 ± 10.2*	21.0 ± 7.1	33.5 ± 8.9
Benzamil, mucosal	3	35.6 ± 12.3*	20.3 ± 4.6	39.0 ± 5.1
Gd_3Cl, serosal	4	111.2 ± 5.15	36.2 ± 1.6	47.2 ± 1.9
La_3Cl, serosal	3	110.3 ± 14.9	28.3 ± 6.7	36.3 ± 7.2
100 μM amiloride, serosal	3	95.5 ± 2.0	24.0 ± 2.4	39.0 ± 5.7
Ca^{2+}				
No apical Ca^{2+}	3	28.3 ± 6.1*	22.6 ± 3.8	34.3 ± 4.3
2-APB	3	54.6 ± 2.6*	30.6 ± 6.1	32.0 ± 6.1
Ryanodine	3	88.3 ± 11.8	32.0 ± 3.3	44.6 ± 3.3
K^+ channels				
NS1619	3	82.0 ± 4.6	34.6 ± 1.4	53.3 ± 3.1
NS309	3	81.6 ± 12.8	44.2 ± 0.3*	76.0 ± 1.5*
Chromakalim	4	94.0 ± 8.1	45.7 ± 2.6*	87.5 ± 3.5*
Arachadonic acid	3	95.7 ± 9.0	32.3 ± 7.5	45.3 ± 5.0
Halothane	3	106.6 ± 0.8	35.3 ± 0.8	48.5 ± 3.7
Glyburide + chromakalim	3	90.6 ± 5.6	32.0 ± 4.5	51.0 ± 6.0
Glyburide	4	85.3 ± 12.7	26.4 ± 7.2	32.6 ± 8.5

Tissue was bowed outward at the indicated pressure head, speed, or temperature or after the indicated treatment. Data are mean ± SEM. C_{max} was measured at the end of phase 1, C_{min} was measured at the end of phase 2, and C_{60} was measured 60 min after initiation of the mechanical stimulus.

[a,b] Data are identical and are reproduced for clarity.

* $p < 0.05$ relative to control.

ing drug latrunculin A caused a decrease in stretch-induced changes in C_T during phases 2 and 3 (Figure 7 and Table 1); however, the effect did not reach statistical significance. Intermediate filaments are physically associated with the discoidal vesicles and apical membrane of umbrella cells, but their function is poorly understood. We observed that treatment with thioglycolic acid, a reagent that reduces disulfide bridges and disorganizes the cytokeratin network (Sarikas and Chlapowski, 1986; Veranic and Jezernik, 2002), inhibited the stretch-induced responses (Figure 7 and Table 1). A similar response was observed upon treatment with okadaic acid, a protein serine/threonine phosphatase inhibitor that is reported to fragment intermediate filaments (Blankson *et al.*, 1995; Figure 7 and Table 1). However, this drug has many effects that are independent of the cytoskeleton (Swingle *et al.*, 2007). In contrast, treatment with the microtubule depolymerizing agent colchicine had no significant effect on C_T (Figure 7 and Table 1). In summary, the early stage exocytic response was dependent on the cytoskeleton, but independent of temperature.

Roles for ENaC, an NSCC, and $[Ca^{2+}]_i$ in the Phase 1 Response to Outward Bowing

Na^+ conductance is a major contributor to I_{sc} in quiescent and stretched umbrella cells (Lewis and Wills, 1983; Wang *et al.*, 2003b), and mathematical modeling showed that Na^+ permeable ion channels, possibly in conjunction with K^+ conducting channels, could account for the phase 1 response of outward bowing (Supplemental Figure S1). We observed

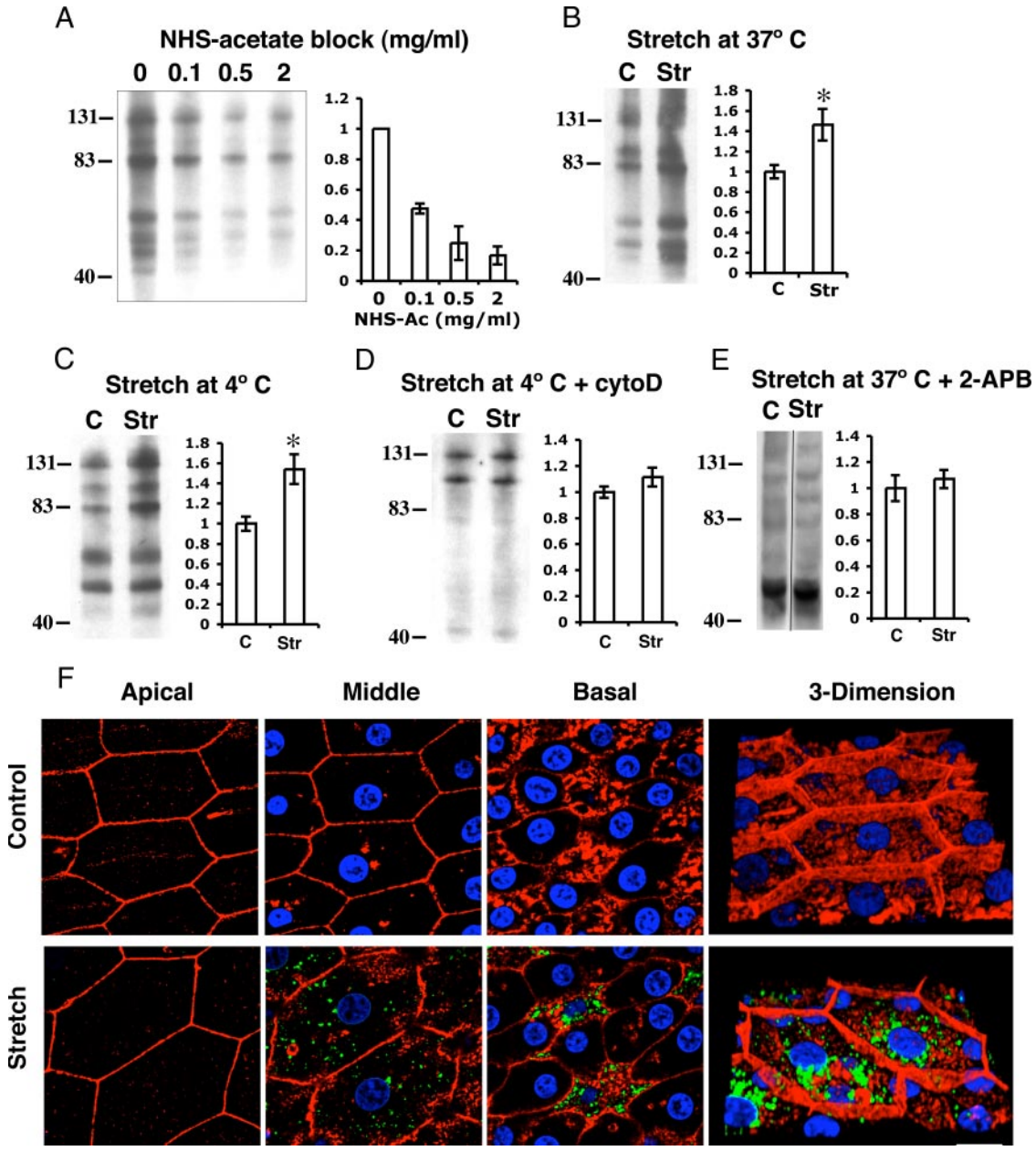

Figure 6. Increased membrane turnover in response to acute changes in hydrostatic pressure. (A) Tissue was mounted, equilibrated, and then cooled to 4°C for 30 min. The apical surface of the cells was treated with the indicated concentration of sulfo-NHS acetate for 60 min, washed, and then incubated with 0.5 mg/ml sulfo-NHS–SS-biotin for 15 min to biotinylate unblocked apical membrane proteins. The percent change in biotinylated proteins way quantified by densitometry and is plotted in the graph to the right. (B and C) The apical surface of the umbrella cells was incubated with 1 mg/ml sulfo-NHS acetate for 60 min at 4°C, and then the tissue was bowed outward (2 cm H_2O pressure using a 20-gauge needle) for 5 min at 37°C (B) or 10 min at 4°C (C). The apical surface of tissue was then incubated with 0.5 mg/ml sulfo-NHS–SS-biotin for 15 min to biotinylate newly inserted apical membrane proteins. The percent change in biotinylated proteins is shown in the panel to the right. (D) The tissue was incubated with 1 mg/ml sulfo-NHS acetate, treated with cytochalasin D for 60 min at 37°C, stretched 10 min at 4°C, and the apical surface biotinylated. The percent change in biotinylated proteins is shown in the panel to the right. (E) Percent change in biotinylated proteins for tissue bowed outward (2 cm H_2O pressure using a 20-gauge needle) at 37°C in the presence of 75 μM 2-APB. (A–E) Data are expressed as mean ± SEM ($n \geq 3$). Representative lysates from control (C) or stretched (Str) samples are shown in B–E. Statistically significant difference (* $p < 0.05$) relative to control. (F) Tissue was mounted, equilibrated, and then cooled to 4°C for 30 min. WGA was added to the mucosal hemichamber and incubated for 30 min, and the tissue was bowed outward for 10 min at 4°C by filling the chamber using a 20-gauge needle at a 2 cm H_2O pressure head. Unstretched tissue served as control. Shown are individual optical sections taken from the apical, middle, and basal regions of stretched umbrella cells. Rhodamine phalloidin was used to label the actin cytoskeleton (red), and Topro-3 was used to label the nuclei (blue). A three-dimensional reconstruction of the cell is shown at the right. Bar, 20 μm.

that, consistent with a role for ENaC in these responses, 1 μM amiloride or 1 μM benzamil (a highly selective inhibitor of ENaC) inhibited the phase 1 response of outward bowing (Figure 8A and Table 1) and benzamil inhibited the stretch-

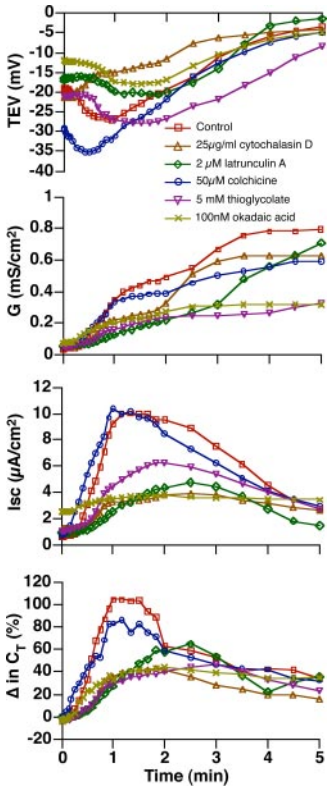

Figure 7. Role of the cytoskeleton in the electrophysiological responses to outward bowing. The tissue was pretreated with the indicated blocker for 30 min at 37° C. The tissue was then bowed outward using a 20-gauge needle to fill the mucosal hemichamber at a 2 cm H_2O pressure head. Untreated tissue served as a control. The experiments were repeated ≥3 times, and representative results are shown.

induced increase in apical membrane turnover ($p > 0.05$; not shown). However, these inhibitors had no effect on the phase 2 or the phase 3 changes in C_T (Table 1). In addition to ENaC, we have also described an apically localized NSCC that may also play an important role in the processes we described (Wang *et al.*, 2003b). In fact, we observed that mucosal addition of 1 mM Gd^{3+} or La^{3+} (inhibitors of the NSCC; Mohanty and Li, 2002; Wang *et al.*, 2003b) or 100 μM amiloride (an inhibitor of both ENaC and the NSCC when used at this concentration; Wang *et al.*, 2003b) impaired the phase 1 response of outward bowing (Figure 8A and Table 1), but had little effect on C_T changes during phase 2 or phase 3 (Table 1). When Gd^{3+}, La^{3+}, or amiloride was added to the serosal hemichamber, they had only small effects on the phase 1 parameters and no significant effects on C_T (Figure 8B and Table 1), further indicating that the basolateral membrane events may be differentially regulated.

NSCCs often conduct extracellular Ca^{2+} into the cell, stimulating Ca^{2+}-dependent increases in $[Ca^{2+}]_i$. Consistent with this possibility we observed that depleting the apical Krebs solution of Ca^{2+} blocked the phase 1 response, but not the phase 2 or 3 responses (Figure 8C and Table 1). Ca^{2+}-dependent Ca^{2+} release can occur downstream of IP_3 receptor or ryanodine receptor activation. We observed that the IP_3 receptor inhibitor 2-APB inhibited the phase 1 response, whereas ryanodine (which inhibits the ryanodine receptor at this concentration) had little effect (Figure 8C and Table 1). Furthermore, 2-APB inhibited the stretch-induced increase in apical membrane turnover (Figure 6E). Although there was some variation in the intensity of the protein bands between 6 A–C, and 6E, this can be attributed to differences in animals/tissue and experimenters. Taken as a whole our data are consistent with the possibility that extracellular Ca^{2+} enters through the apical pole of the cell and stimulates $[Ca^{2+}]_i$ downstream of an IP_3-receptor–dependent pathway.

Basolateral K^+ Channels Modulate Stretch-induced Responses in Umbrella Cells

We previously reported that stretch-sensitive K^+ channels are present on the basolateral surface of umbrella cells (Wang *et al.*, 2003b). RT-PCR of uroepithelial-derived mRNA was used to identify 10 possible stretch-modulated K^+ channels that are expressed in the bladder. Nine of them were detected in uroepithelium, including the calcium-activated potassium channels KCNMA1 (BK) and KCNN1-4 (SK/IK), the two-pore potassium channels KCNK2 (TREK-1) and KCNK4 (TRAAK), and the inwardly rectifying potassium channels KCNJ8 (Kir6.1) and KCNJ11 (Kir6.2). Only KCNK10 (TREK-2) was not detected in the uroepithelium (Figure 9A); however, we confirmed that its expression was detected in the heart (data not shown). Kir6.1 and Kir6.2 are subunits of ATP-sensitive potassium channels (K_{ATP} channels). K_{ATP} has important roles in bladder function and can regulate membrane traffic in other cell types (Bonev and Nelson, 1993; Gopalakrishnan *et al.*, 1999; Henquin, 2004). To further establish that K_{ATP} was expressed in the uroepithelium and to determine its localization in umbrella cells, Western blots and immunofluorescence were performed using antibodies against Kir6.1. Western blot analysis confirmed the expression of an expected 44.7-kDa protein species (Figure 9B). Furthermore, immunofluorescence staining showed expression of Kir6.1 in the uroepithelium, including at the basolateral membrane of the umbrella cell layer (Figure 9C).

The mathematical model shown in Supplemental Figure S1 predicts that opening K^+ channels at the basolateral surface of the umbrella cells may effect the phase 2 and possibly phase 3 responses upon outward bowing. We used K^+ channel openers to determine which K^+ channel(s) was functional in modulating the stretch-induced umbrella cell response. NS1619, a potent BK opener, had no effect on stretch-induced responses (Figure 9D and Table 1). Arachidonic acid or halothane, which open channels such as TREK-1 and TRAAK, also had no effect (Figure 9D and Table 1). In contrast, the SK/IK channel opener NS309 modulated the phase 2 and 3 responses and increased the magnitude of the TEV, conductance, and C_T (Figure 9D and Table 1). We also observed that cromakalim, a K_{ATP} channel opener, changed the stretch-induced responses in a manner similar to NS309 (Figure 9D and Table 1). Glyburide, a K_{ATP} inhibitor, blocked the cromakalim effect (Table 1); however, glyburide itself had no effect on the stretch responses (Table 1). Our data indicate that SK/IK and K_{ATP} may modulate the basolateral membrane responses to umbrella cell stretch.

DISCUSSION

Several insights have emerged from our studies of umbrella cell mechanotransduction: First, stretch, not pressure, is the relevant mechanical stimulus that regulates ion and membrane transport in the umbrella cell. Second, during the early stage (i.e., phase 1 and 2 responses to outward bowing) the apical and basolateral membranes of the umbrella cell may have discrete functions that act in concert to regulate membrane turnover at the apical surface of the umbrella cell. In contrast, the late stage (i.e., phase 3 response to outward bowing) appears to reflect the responses of umbrella cells

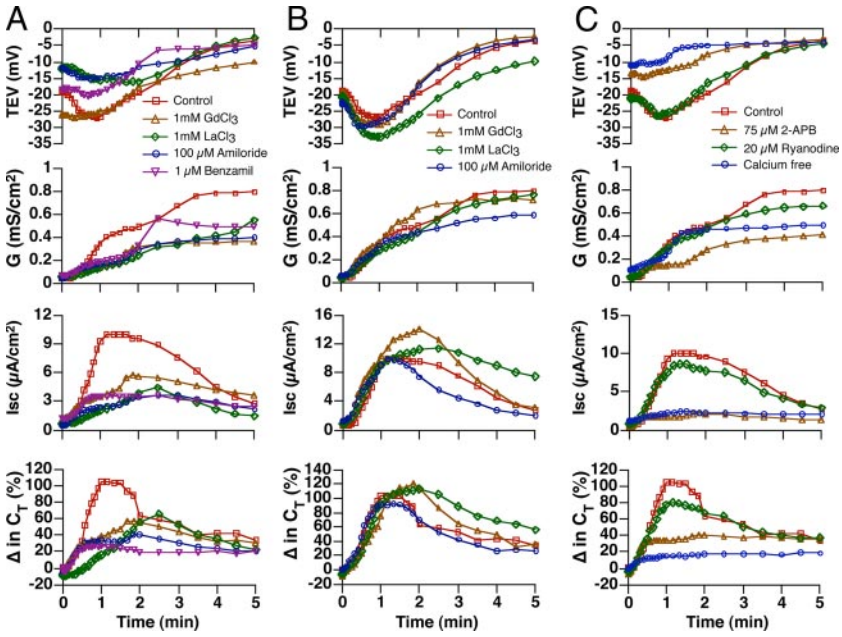

Figure 8. Requirement for apical membrane cation channels and intracellular Ca^{2+} release in the phase 1 response to outward bowing. (A and B) The indicated channel blockers were added to the mucosal (A) or serosal (B) hemichamber and preincubated for 30 min at 37°C. The tissue was then bowed outward using a 20-gauge needle to fill the mucosal hemichamber at a 2 cm H_2O pressure head. (C) Tissue was pretreated with 2-APB or ryanodine for 1 h and then stretched as described in A and B. Alternatively, the apical solution was exchanged for one lacking Ca^{2+}, and the tissue was stretched. In A-C untreated tissue served as a control and is reproduced from Figure 7. The experiments were repeated ≥3 times, and representative results are shown.

that have reached a mechanical equilibrium, when the uroepithelium is fully bowed outward and tension is present in both umbrella cell membranes. Third, we established that during the early stage, ion channels likely act as mechanotransducers to regulate changes in umbrella cell apical membrane traffic. Fourth, the responses we observed may be physiologically relevant to the dynamic processes of bladder filling and voiding. Overall our results provide increased understanding of how changes in the mechanical environment of umbrella cells are transduced by discrete membrane domains to coordinate ion transport and membrane traffic.

Role of Stretch in Promoting Changes in Umbrella Cell Function

Previous studies have established that umbrella cells are mechanosensitive and in response to mechanical stimuli

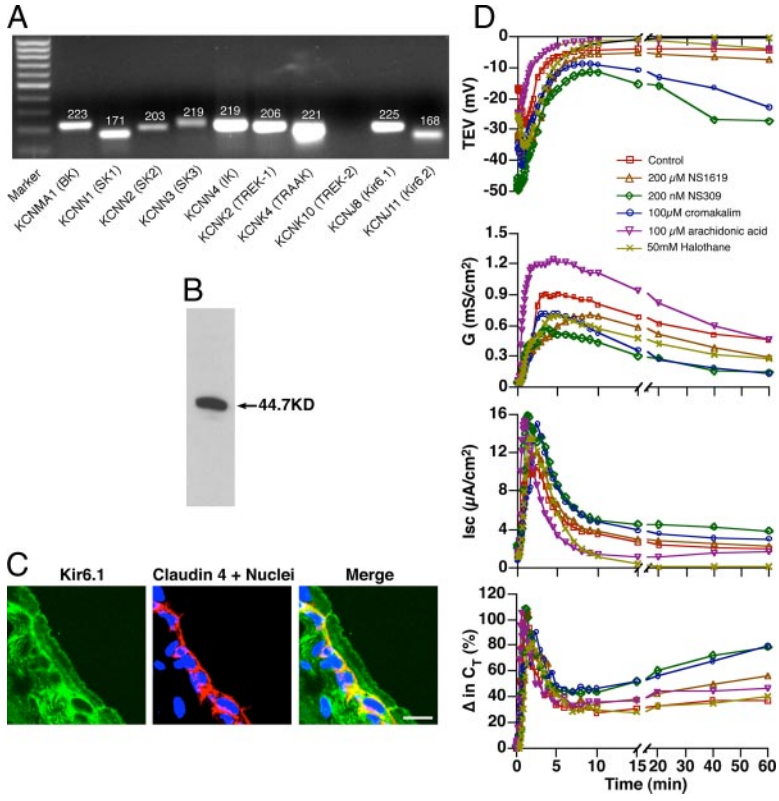

Figure 9. K_{ATP} is expressed in umbrella cells and modulates the stretch response. (A) Expression of the indicated K^+ channels was detected by RT-PCR of total RNA isolated from mouse bladder uroepithelium. Numbers above the DNA species are the expected product sizes of the RT-PCR reaction (in base pairs). (B) A lysate of rat uroepithelium was resolved by SDS-PAGE and a Western blot probed with antibody specific for the Kir6.1 subunit of K_{ATP}. The nominal mass of the major protein detected in the lysate is indicated to the right of the panel. (C) Frozen thin sections of rat bladder tissue were labeled with an antibody to the Kir6.1 subunit of K_{ATP} (green), claudin-4 (red) to label the basolateral membranes of the umbrella cells and plasma membranes of the underling intermediate and basal cells and Topro-3 to label the cell nuclei (blue). A merged panel is shown at the right. Bar, 10 μm. (D) The indicated K^+ channel openers were added to the serosal hemichamber and incubated with tissue for 30 min. The tissue was then bowed outward by filling the chamber with a 20-gauge needle at a 2 cm H_2O pressure head. The experiments were repeated ≥3 times, and representative results are shown.

show increased ion transport (Lewis and de Moura, 1982; Wang *et al.,* 2003b), apical membrane turnover (exocytosis and endocytosis; Lewis and de Moura, 1982; Truschel *et al.,* 2002; Wang *et al.,* 2003a), and release of various mediators and neurotransmitters including ATP and adenosine (Ferguson *et al.,* 1997; Lewis and Lewis, 2006; Yu *et al.,* 2006). We observed that increased membrane tension (i.e., stretch) and not pressure was likely responsible for stimulating these changes. Stretch, but not pressure, was previously reported to open the MscL channel (Moe and Blount, 2005) and to increase endothelial connexin 43 expression (Kwak *et al.,* 2005). In a similar manner, stretch of the apical or basolateral membranes of umbrella cells may modulate ion channel activities that regulate apical membrane transport. While increased membrane tension (i.e., stretch) may be the physiologically relevant stimulus in these and other cells, it is possible that pressure itself may play some role in other responses.

Distinct Effects of Increasing Apical or Basolateral Membrane Tension on Umbrella Cell Apical Membrane Traffic

In this and previous studies we observed that the late stage response was inhibited by temperature and BFA (Truschel *et al.,* 2002; Balestreire and Apodaca, 2007), but was unaffected by apical membrane channel blockers. In contrast the early stage exocytic events we studied were triggered by increases in apical membrane tension and could be blocked by agents that perturbed the cytoskeleton, prevented rises in $[Ca^{2+}]_i$, or inhibited apical membrane channel function (see *Discussion*). We further observed that the early stage response was modulated by endocytosis, which was stimulated by increased basolateral membrane tension, occurred after the first phase of outward bowing and predominated during the second phase of this response. In neurons and neuroendocrine cells exocytic bursts are often followed by a compensatory endocytosis, which modulates the increase in plasma membrane surface area, regulates signaling responses, and recovers protein machinery needed for additional rounds of exocytosis (Barg and Machado, 2008). Presumably the endocytosis we observed in umbrella cells plays similar functions. Compensatory endocytosis in neuroendocrine cells is typically rapid, is initiated by Ca^{2+} entry into the cell, and is modulated by phosphorylation and dynamin-1, but not clathrin (Barg and Machado, 2008). Our results indicate that compensatory endocytosis in umbrella cells depend on increased basolateral membrane tension and may be modulated by K^+ channels (see *Discussion*).

Intriguingly, early stage exocytic events were not sensitive to treatment with BFA and were independent of temperature. Membrane trafficking events are generally thought to be temperature sensitive, which reflects changes in protein folding and lipid fluidity at low temperatures as well as the presence of a thermodynamic barrier that is not conducive to membrane traffic. However, endocytosis of some viral proteins is only partially inhibited at 4°C, and exocytosis is observed in garter snake nerve terminals, the *Xenopus* pars intermedia, and the type II pneumocytes of hibernating squirrels at reduced temperatures (Elliot and O'Hare, 1997; Ormond *et al.,* 2003; Tonosaki *et al.,* 2004; Rentsendorj *et al.,* 2005; Richard *et al.,* 2005; Teng and Wilkinson, 2005). These studies indicate that exocytosis/endocytosis are not fundamentally impossible at reduced temperatures. Although rabbit umbrella cells are unlikely to experience cold temperatures under normal conditions, membrane traffic in these cells may be somewhat insensitive to cold temperatures because the mechanical energy provided by stretching the tissue is sufficient to overcome the normal energy barrier that slows exocytosis/endocytosis in mammalian cells incubated at 4°C.

Early investigators posited that the highly pleated apical plasma membrane of the umbrella cell simply unfolds during bladder filling (Koss, 1969; Staehelin *et al.,* 1972). If true, the changes in capacitance we measured may result from the unfurling of apical membrane pockets or adhesions that in their folded state would be tight to ions and other small molecules. However, it is difficult to reconcile this model with our findings that the early stage capacitance changes were blocked by treatments as varied as depletion of apical Ca^{2+} and inhibition by APB, channel blockers, and agents that disrupt the cytoskeleton. In addition, we previously examined the ultrastructure of serially sectioned tissue to show that when uroepithelial tissue is mounted on tissue rings, the apical surface of umbrella cells contains no detectable pockets/adhesions and the subapical pool of discoidal vesicles are not continuous with the plasma membrane (Truschel *et al.,* 2002). Furthermore we have performed numerous biochemical studies that show that stretch-induced increases in surface area are a result of fusion of discoidal/fusiform-shaped vesicles with the apical plasma membrane of the umbrella cell and not simply unfolding of apical membrane (Truschel *et al.,* 2002; Apodaca, 2004; Khandelwal *et al.,* 2008).

If discoidal/fusiform vesicles are important for both the early stage and late stage responses, then what accounts for the differences in the regulation of these processes? We suggest that the early stage events may reflect trafficking of a preexisting pool of vesicles. We observed that, consistent with this possibility, the early stage changes in surface area can occur on a rapid time scale and do not require new protein synthesis or secretion (Truschel *et al.,* 2002; Balestreire and Apodaca, 2007). In contrast, the timing of the late stage events and their dependence on protein synthesis and secretion indicate that are likely mediated by a newly synthesized pool of vesicles. Further exploration is required to understand the relationship of the two exocytic responses, the membrane pools involved in these two processes and how they are regulated.

Regulation of Umbrella Cell Apical Membrane Traffic by Ion Channels

Like those in other cells (Laine *et al.,* 1994; Kim *et al.,* 1997; Jiao *et al.,* 2000), stretch-modulated channels may act as mechanotransducers to signal increased exocytosis at the apical surface of the umbrella cell. Likely candidates include an NSCC and ENaC. In response to stretch, the NSCC may conduct apical Ca^{2+}, which could stimulate exocytosis directly or indirectly by promoting Ca^{2+}-dependent Ca^{2+} release from IP_3-receptor dependent stores in the endoplasmic reticulum (Figure 10). In addition $[Ca^{2+}]_i$ could also allow for cross-talk between the apical channels and basolateral K^+ channels (e.g., see Sand *et al.,* 2004), which we also showed may play a regulatory role in modulating the exocytic response. As well, K^+ channels are known to modulate Ca^{2+} responses in cells (Henquin, 2004). The identity of the NSCC is unknown; however, members of the TRP family of proteins such as polycystin 1/2 may be candidates, as polycystin 1 is expressed in the uroepithelium (Ibraghimov-Beskrovnaya *et al.,* 1997).

Ferguson and coworkers previously proposed that ENaC may act as a mechanosensor to regulate ATP release from the uroepithelium (Ferguson, 1999), and data from other cell types indicates that ENaC activity may be triggered by membrane stretch (Lewis and de Moura, 1982; Ferguson

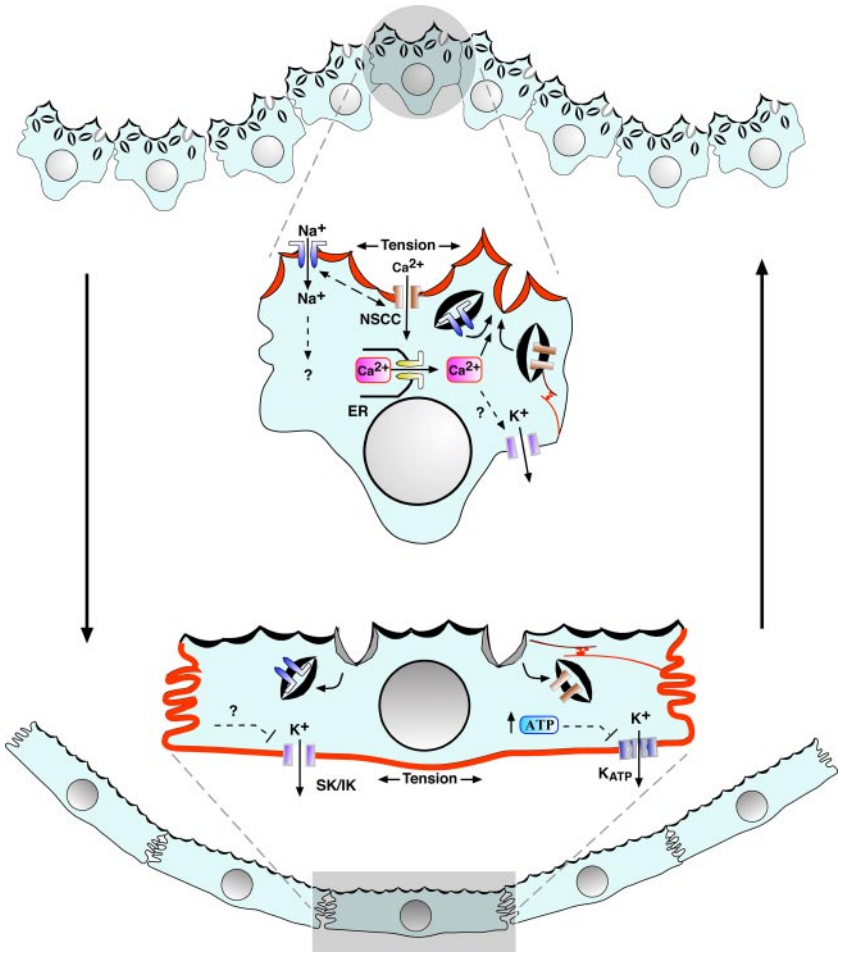

Figure 10. Model for stretch-induced umbrella cell responses. As the bladder fills, the folded mucosal surface of the bladder is pushed outward, and increased tension at the apical membrane causes opening of an NSCC, stimulating influx of extracellular Ca^{2+}. The increased $[Ca^{2+}]_i$ triggers Ca^{2+}-dependent Ca^{2+} release from IP_3 dependent stores, which stimulates exocytosis and may modulate the activity of other channels. Exocytosis may amplify the initial response by stimulating delivery of additional stretch sensing channels to the apical surface of the cell. ENaC, perhaps acting downstream of the NSCC, is also opened and may modulate the exocytic response by changing the membrane potential or the driving force for the entry of other ions (e.g., by modulating the activity of the Na^+,K^+ ATPase). As the epithelium bows further outward, tension in the basolateral membrane would further increase. This would cause an increase in apical membrane endocytosis, which would modulate the exocytic response by stimulating internalization of apical membrane channels and other sensory molecules (not shown). The mechanosensor at this membrane is unknown but may include the cytoskeleton and associated integrins (not shown) or stretch-modulated K^+ channel(s), which may close in response to the increased tension or other intracellular mediators such as ATP. During voiding, tension would increase in the basolateral membrane as the mucosa refolds. The increased tension would further stimulate endocytosis of apical membrane and its constituents, readying the umbrella cell for the next cycle of filling. For clarity we do not include the underlying cell layers or connective tissue; however, they may contribute to the events in the overlying umbrella cell layer by release of mediators and effects on umbrella cell tension.

et al., 1997; Carattino *et al.*, 2004; Althaus *et al.*, 2007). Our data indicate that ENaC, acting downstream or in conjunction with the NSCC, could play a role in mechanotransduction by modulating membrane potential or cross-talk between ion channels at the apical and basolateral membrane domains. We do not know if there are additional mechanotransducers that act upstream of NSCC and ENaC. In this regard, apical membrane stretch is likely to increase tension in the underlying cytoskeleton and this will lead to activation of integrins, which not only modulate cytoskeletal tension but may also play important roles in initiating and/or propagating signaling responses at the apical surface of epithelial cells (Ingber, 2003; Alenghat *et al.*, 2004).

We do not know the identity of the mechanotransduction pathway(s) that functions at the basolateral surface of the umbrella cell to regulate apical endocytosis. One possibility is that it involves the closing of one or more basolaterally localized K^+ channels including SK/IK and/or K_{ATP}. Intriguingly, our data showed that openers of these channels may modulate the second and third phases of outward bowing and that both openers stimulated a significant elevation in C_T. The increase may represent a slowing in the endocytic rate or an increase in exocytic rate. Additional mechanosensors may include the actomyosin cytoskeleton, which in conjunction with integrins is required for mechanosensation in both anchored and nonanchored cells (Gillespie and Walker, 2001; Frey *et al.*, 2006; Ingber, 2006; Effler *et al.*, 2007) and is prominently associated with the basolateral membrane of the umbrella cell (Acharya *et al.*, 2004). Treatment with cytochalasin D or latrunculin impairs exocytosis and endocytosis in umbrella cells (Lewis and de Moura, 1982). Although this may reflect effects on discoidal/fusiform vesicle dynamics, it is plausible that it may also result from defects in mechanotransduction and cytoskeletal tension regulation.

Physiological Relevance of the Early and Late Stage Responses

The bladder fills in a multiphase manner. An initial filling phase, marked by a rapid rise in pressure to 2–5 cm H_2O, is followed by a long storage phase, when the pressure rises only slowly. The subsequent micturition phase is characterized by rapid spikes in bladder pressure (which can rise to >100 cm H_2O) as the smooth muscle contracts, and ultimately terminates with voiding. We suggest that the early stage events we described may be important to all three phases of bladder filling. In the filling and storage phases the uroepithelium is in a dynamic mechanical state as the mucosa is actively unfolding and is slowly bowed outward in response to increased urine volume, whereas in the micturition phase the epithelium must maintain patency in the face of rapid pressure changes. In all cases the increase in apical surface area would help dissipate the pressure (allowing the cells to maintain their barrier function) and stimulate the surface expression of apical membrane channels and receptors that would sense bladder filling as well as urine contents (sensory function). Increases in basolateral tension would modulate the apical membrane responses by stimu-

lating endocytosis. The increases in apical and/or basolateral tension may signal the onset of the late stage, likely by stimulating the activation of the epidermal growth factor receptor (Balestreire and Apodaca, 2007). The late-stage response may be important during the middle to late portions of the storage phase, when the mucosa is bowed outward and must accommodate the increasing urinary volume. The dual-membrane response we observed during the early stage is not only relevant to bladder filling, but may also be important for the relatively rapid process of bladder voiding. On release of the bladder contents, the epithelium is rapidly refolded, which would dissipate any apical membrane tension. Furthermore, it would also likely increase tension at the basolateral surface of the uroepithelial cells in the forming crest regions of the folds, which would be actively pushed by the underlying matrix and musculature toward the lumen of the bladder. As we observed, increased tension in the basolateral surface of the umbrella cells would promote endocytosis of membrane and associated sensory receptors and channels, returning the umbrella cell layer to its basal state before another cycle of bladder filling. Finally, we note that the umbrella cells likely transmit tension to the interconnected matrix, as well as to the underlying intermediate and basal cell layers and they, in turn, may impact or promote events in the overlying umbrella cell layer by release of mediators and modulation of tension across the uroepithelium.

Summary and Model

We propose a model in which the polarized membrane domains of the umbrella cell act in concert to regulate apical membrane dynamics in this cell during bladder filling and voiding (Figure 10). Although increased tension in the apical membrane of the umbrella cell stimulates opening of stretch-sensitive channels that induce exocytosis, subsequent increases in tension across the basolateral membrane stimulate apical membrane endocytosis. The latter process would ensure membrane turnover and would act in combination with exocytosis to modulate the sensory and barrier functions of the epithelium as the bladder fills and empties. It likely that the mechanisms we observe in umbrella cells will apply to other mechanically sensitive epithelial cells (e.g., those that line the urinary tract, gastrointestinal tract, respiratory tract, and vascular system), whose distinct membrane domains likely also act in concert to modulate the function of these cells and their end organs.

ACKNOWLEDGMENTS

We thank Drs. Hallows, Hawryluk, Johnson, and Traub for their insightful comments during the preparation of this manuscript. We also thank Dr. Lin for helping us with the mathematical modeling of ion transport in umbrella cells and Wily G. Ruiz for his excellent technical support in completing the biotin experiments. This work was supported by an American Heart Association Predoctoral Fellowship (W.Y.), a postdoctoral fellowship from the National Kidney Foundation (P.K.), and National Institutes of Health (NIH) Grant R37-DK54425 (G.A.), and in part by the NIH-sponsored Pittsburgh Center for Kidney Research Grant P30 DK079307.

REFERENCES

Acharya, P., Beckel, J., Ruiz, W. G., Wang, E., Rojas, R., Birder, L., and Apodaca, G. (2004). Distribution of the tight junction proteins ZO-1, occludin, and claudin-4, -8, and -12 in bladder epithelium. Am. J. Physiol. Renal Physiol. *287*, F305–F318.

Alenghat, F. J., Nauli, S. M., Kolb, R., Zhou, J., and Ingber, D. E. (2004). Global cytoskeletal control of mechanotransduction in kidney epithelial cells. Exp. Cell Res. *301*, 23–30.

Althaus, M., Bogdan, R., Clauss, W. G., and Fronius, M. (2007). Mechanosensitivity of epithelial sodium channels (ENaCs): laminar shear stress increases ion channel open probability. FASEB J. *21*, 2389–2399.

Apodaca, G. (2002). Modulation of membrane traffic by mechanical stimuli. Am. J. Physiol. Renal Physiol. *282*, F179–F190.

Apodaca, G. (2004). The uroepithelium: not just a passive barrier. Traffic *5*, 117–128.

Balestreire, E. M., and Apodaca, G. (2007). Apical EGF receptor signaling: regulation of stretch-dependent exocytosis in bladder umbrella cells. Mol. Biol. Cell *18*, 1312–1323.

Barg, S., and Machado, J. D. (2008). Compensatory endocytosis in chromaffin cells. Acta Physiol. *192*, 195–201.

Blankson, H., Holen, I., and Seglen, P. O. (1995). Disruption of the cytokeratin cytoskeleton and inhibition of hepatocytic autophagy by okadaic acid. Exp. Cell Res. *218*, 522–530.

Bonev, A. D., and Nelson, M. T. (1993). ATP-sensitive potassium channels in smooth muscle cells from guinea pig urinary bladder. Am. J. Physiol. *264*, C1190–C1200.

Carattino, M. D., Sheng, S., and Kleyman, T. R. (2004). Epithelial Na^+ channels are activated by laminar shear stress. J. Biol. Chem. *279*, 4120–4126.

Effler, J. C., Iglesias, P. A., and Robinson, D. N. (2007). A mechanosensory system controls cell shape changes during mitosis. Cell Cycle *6*, 30–35.

Elliot, G., and O'Hare, P. (1997). Intercellular trafficking and protein delivery by a herpesvirus structural protein. Cell *88*, 223–233.

Ferguson, D. R. (1999). Urothelial function. B.J.U. Int. *84*, 235–242.

Ferguson, D. R., Kennedy, I., and Burton, T. J. (1997). ATP is released from rabbit urinary bladder epithelial cells by hydrostatic pressure changes—a possible sensory mechanism? J. Physiol. *505*(Pt 2), 503–511.

Frey, M. T., Tsai, I. Y., Russell, T. P., Hanks, S. K., and Wang, Y. L. (2006). Cellular responses to substrate topography: role of myosin II and focal adhesion kinase. Biophys. J. *90*, 3774–3782.

Gillespie, P. G., and Walker, R. G. (2001). Molecular basis of mechanosensory transduction. Nature *413*, 194–202.

Gopalakrishnan, M. *et al.* (1999). Characterization of the ATP-sensitive potassium channels (KATP) expressed in guinea pig bladder smooth muscle cells. J. Pharmacol. Exp. Ther. *289*, 551–558.

Henquin, J.C. (2004). Pathways in beta-cell stimulus-secretion coupling as targets for therapeutic insulin secretagogues. Diabetes *53*(Suppl. 3), S48–S58.

Ibraghimov-Beskrovnaya, O. *et al.* (1997). Polycystin: in vitro synthesis, in vivo tissue expression, and subcellular localization identifies a large membrane-associated protein. Proc Natl Acad Sci USA *94*, 6397–6402.

Ingber, D. E. (2003). Tensegrity II. How structural networks influence cellular information processing networks. J. Cell Sci. *116*, 1397–1408.

Ingber, D. E. (2006). Cellular mechanotransduction: putting all the pieces together again. FASEB J. *20*, 811–827.

Jiao, J. H., Baumann, P., Baron, A., Roatti, A., Pence, R. A., and Baertschi, A. J. (2000). Sulfonylurea receptor ligands modulate stretch-induced ANF secretion in rat atrial myocyte culture. Am. J. Physiol. Heart Circ. Physiol. *278*, H2028–H2038.

Khandelwal, P., Ruiz, G., Balestreire-Hawryluk, E., Weisz, O. A., and Goldenring, J. A. (2008). Rab11a-dependent exocytosis of discoidal/fusiform vesicles in bladder umbrella cells. Proc. Natl. Acad. Sci. USA *105*, 15773–15778.

Kim, S. H., Cho, K. W., Chang, S. H., Kim, S. Z., and Chae, S. W. (1997). Glibenclamide suppresses stretch-activated ANP secretion: involvements of K^+ATP channels and L-type Ca^{2+} channel modulation. Pfluegers Arch. *434*, 362–372.

Koss, L. G. (1969). The asymmetric unit membranes of the epithelium of the urinary bladder of the rat: an electron microscopic study of a mechanism of epithelial maturation and function. Lab. Invest. *21*, 154–168.

Kwak, B. R., Silacci, P., Stergiopulos, N., Hayoz, D., and Meda, P. (2005). Shear stress and cyclic circumferential stretch, but not pressure, alter connexin43 expression in endothelial cells. Cell Commun. Adhes. *12*, 261–270.

Laine, M., Arjamaa, O., Vuolteenaho, O., Ruskoaho, H., and Weckstrom, M. (1994). Block of stretch-activated atrial natriuretic peptide secretion by gadolinium in isolated rat atrium. J. Physiol. *480*, 553–561.

Lewis, S., and de Moura, J. (1984). Apical membrane area of rabbit urinary bladder increases by fusion of intracellular vesicle: an electrophysiological study. J. Membr. Biol. *82*, 123–136.

Lewis, S. A., and de Moura, J. L. (1982). Incorporation of cytoplasmic vesicles into apical membrane of mammalian urinary bladder epithelium. Nature *297*, 685–688.

Lewis, S. A., Eaton, D. C., Clausen, C., and Diamond, J. M. (1977). Nystatin as a probe for investigating the electrical properties of a tight epithelium. J. Gen. Physiol. *70*, 427–440.

Lewis, S. A., and Hanrahan, J. W. (1990). Physiological approaches for studying mammalian urinary bladder epithelium. Methods Enzymol. 192, 632–650.

Lewis, S. A., and Lewis, J. R. (2006). Kinetics of urothelial ATP release. Am. J. Physiol. Renal. Physiol. *291*, F332–F340.

Lewis, S. A., and Wills, N. K. (1983). Apical membrane permeability and kinetic properties of the sodium pump in rabbit urinary bladder. J. Physiol. *341*, 169–184.

Moe, P., and Blount, P. (2005). Assessment of potential stimuli for mechano-dependent gating of MscL: effects of pressure, tension, and lipid headgroups. Biochemistry *44*, 12239–12244.

Mohanty, M. J., and Li, X. (2002). Stretch-induced Ca(2+) release via an IP(3)-insensitive Ca(2+) channel. Am. J. Physiol. Cell Physiol. *283*, C456–C462.

Ormond, C. J., Orgeig, S., Daniels, C. B., and Milsom, W. K. (2003). Thermal acclimation of surfactant secretion and its regulation by adrenergic and cholinergic agonists in type II cells isolated from warm-active and torpid golden-mantled ground squirrels, *Spermophilus lateralis*. J. Exp. Biol. *206*, 3031–3041.

Rentsendorj, A., Agadjanian, H., Chen, X., Cirivello, M., Macveigh, M., Kedes, L., Hamm-Alvarez, S., and Medina-Kauwe, L. K. (2005). The Ad5 fiber mediates nonviral gene transfer in the absence of whole virus, utilizing a novel cell entry pathway. Gene Ther. *12*, 225–237.

Richard, J. P., Melikov, K., Brooks, H., Prevot, P., Lebleu, B., and Chernomordik, L. V. (2005). Cellular uptake of unconjugated TAT peptide involves clathrin-independent endocytosis and heparan sulfate receptors. J. Biol. Chem. *280*, 15300–15306.

Sand, P., Anger, A., and Rydqvist, B. (2004). Hypotonic stress activates an intermediate conductance K^+ channel in human colonic crypt cells. Acta Physiol. Scand. *182*, 361–368.

Sarikas, S. N., and Chlapowski, F. J. (1986). Effect of ATP inhibitors on the translocation of luminal membrane between cytoplasm and cell surface of transitional epithelial cells during the expansion-contraction cycle of the rat urinary bladder. Cell Tissue Res. *246*, 109–117.

Staehelin, L., Chlapowski, F., and Bonneville, M. (1972). Lumenal plasma membrane of the urinary bladder I. Three-dimensional reconstruction from freeze-etch images. J. Cell Biol. *53*, 73–91.

Swingle, M., Ni, L., and Honkanen, R. E. (2007). Small-molecule inhibitors of ser/thr protein phosphatases, use and common forms of abuse. Methods Mol. Biol. *365*, 23–38.

Teng, H., and Wilkinson, R. S. (2005). Clathrin-mediated endocytosis in snake motor terminals is directly facilitated by intracellular Ca^{2+}. J. Physiol. *565*, 743–750.

Tonosaki, Y., Cruijsen, P.M.J.M., Nishiyama, K., Yaninuma, H., and Roubos, E. W. (2004). Low temperature stimulates alpha-melanophore-stimulating hormone secretion and inhibits background adaptation in *Xenopus laevis*. J. Neuroendocrinol. *16*, 894–905.

Truschel, S. T., Wang, E., Ruiz, W. G., Leung, S. M., Rojas, R., Lavelle, J., Zeidel, M., Stoffer, D., and Apodaca, G. (2002). Stretch-regulated exocytosis/endocytosis in bladder umbrella cells. Mol. Biol. Cell *13*, 830–846.

Veranic, P., and Jezernik, K. (2002). Trajectorial organisation of cytokeratins within the subapical region of umbrella cells. Cell Motil. Cytoskelet. *53*, 317–325.

Wang, E., Truschel, S., and Apodaca, G. (2003a). Analysis of hydrostatic pressure-induced changes in umbrella cell surface area. Methods *30*, 207–217.

Wang, E. C., Lee, J. M., Johnson, J. P., Kleyman, T. R., Bridges, R., and Apodaca, G. (2003b). Hydrostatic pressure-regulated ion transport in bladder uroepithelium. Am. J. Physiol. Renal. Physiol. *285*, F651–F663.

Wang, E. C., Lee, J. M., Ruiz, W. G., Balestreire, E. M., von Bodungen, M., Barrick, S., Cockayne, D. A., Birder, L. A., and Apodaca, G. (2005). ATP and purinergic receptor-dependent membrane traffic in bladder umbrella cells. J Clin. Invest. *115*, 2412–2422.

Yu, W., Zacharia, L. C., Jackson, E. K., and Apodaca, G. (2006). Adenosine receptor expression and function in bladder uroepithelium. Am. J. Physiol. Cell Physiol. *291*, C254–C265.